ChemPubSoc Europe
DOI: 10.1002/chem.201502607
CHEMISTRY
A European Journal
Full Paper

Photochemistry |*Hot Paper*|

Photodriven Multi-electron Storage in Disubstituted Ru^{II} Dppz Analogues

Joseph M. Aslan, David J. Boston, and Frederick M. MacDonnell*[a]

Abstract: Four derivatives of the laminate acceptor ligand dipyrido-[3,2-a:2′,3′-c]phenazine (dppz) and their corresponding ruthenium complexes, $[Ru(phen)_2(dppzX_2)]^{2+}$, were prepared and characterized by NMR spectroscopy, ESI-MS, and elemental analysis. The new ligands, generically denoted $dppzX_2$, were symmetrically disubstituted on the distal benzene ring to give 10,13-dibromodppz (dppz-*p*-Br), 11,12-dibromodppz (dppz-*o*-Br), 10,13-dicyanodppz (dppz-*p*-CN), 11,12-dicyanodppz (dppz-*o*-CN). Solvated ground state MO calculations of the ruthenium complexes reveal that these electron-withdrawing substituents not only lower the LUMO of the dppz ligand ($dppz(CN)_2 < dppzBr_2 < dppz$), but that the *para* disubstitution results in a lower LUMO than the *ortho* disubstitution (dppz-*p*-CN < (dppz-*o*-CN), and dppz-*p*-Br < dppz-*o*-Br). The validity of the calculations was confirmed experimentally using cyclic voltammetry. Of the complexes evaluated in this study, only the dicyanodppz complexes showed multiple dppz-based reductions prior to reduction of the phen ligands. The capacity to form singly and doubly reduced dppz-based anions at modest reduction potentials was confirmed using a combination of spectroelectrochemical and chemical titration methods. When subjected to photolysis with visible light in the presence of a sacrificial donor, such as triethylamine, both cyano complexes showed multi-electron reduction. The other complexes only show a single reduction.

Introduction

Compounds that store light energy in the form of high potential electrons are sought after materials.[1] Of the various electron storage systems, ruthenium polypyridal complexes have attracted much attention due to their unique photophysical, optical, and electronic properties, which are useful for potential photocatalytic applications such as H_2 production through single and multi-electron storage. Coincidentally, these complexes are also studied for their interesting DNA binding properties and biological activity.[2]

Ru^{II} polypyridal complexes are commonly utilized in light energy conversion schemes, due to their stability and long-lived excited state lifetimes, which upon reductive quenching, effectively traps an electron in a high energy orbital. In recent years, Ru^{2+} multi-electron storage systems such as $[(phen)_2Ru(tatpp)Ru(phen)_2]^{4+}$ (**P**) and $[(phen)_2Ru(tatpq)Ru(phen)_2]^{4+}$ (**Q**; where phen is 1,10-phenanthroline, tatpp is 9,11,20,22-tetraaza tetrapyrido[3,2-a:2′3′-c:3′′,2′′-l:2′′′,3′′′-n]-pentacene and tatpq is 9,11,20,22-tetraazatetrapyrido[3,2-a:2′3′-c:3′′,2′′-l:2′′′,3′′′-n]-pentacene-10,21-quinone) have been shown to store up to 2 or 4 electrons, respectively, during irradiation with visible light in the presence of a sacrificial donor.[3]

Unfortunately, the potential of the stored electrons in **P** and **Q** are too low (ca. 0 V vs. NHE) to drive important fuel-making reactions, such as proton reduction to H_2. If these complexes are to be used effectively in solar-fuel making processes, it is important not only to store multiple electrons, but also to do so at more negative potentials.

We have attempted to increase the reducing potential of **P** by "bending" the tatpp ligand.[4] This structural modification results in a shift of the first reduction potential by approximately −500 mV showing it is possible to raise the LUMO energy relative to that seen in **P**. This complex, like **P**, also undergoes a second photoreduction but at a significantly slower pace than seen with **P**. Unfortunately, the "bending" of the tatpp ligand seems to increase accessibility of the central portion of the ligand to radical dimerization reactions, which limits the utility of this complex as a photoreduction catalyst. Addition of electron-donating methoxy substituents to the central benzene in the **P** complex also raised the energy of the LUMO significantly, but the resulting complex photochemically eliminates the methoxy substituents during photolysis.[5]

$[Ru(phen)_2dppz]^{2+}$ or $[Ru(bpy)_2dppz]^{2+}$ (phen = 1,10-phenanthroline; bpy = 2,2′-bipyridine; dppz = dipyrido-[3,2-a:2′,3′-c]phenazine) both undergo reductive quenching with sacrificial donors when irradiated, storing a single electron at approximately −0.7 V versus NHE.[6] No doubly reduced products have ever been observed. Fees et al. showed that the reduction potential of $[Ru(bpy)_2(11,12\text{-dimethyl-dppz})]^{2+}$ was shifted approximately 100 mV more negative, signifying a destabilization of the LUMO orbital by electron donating methyl groups. Conversely, electron-withdrawing groups (EWGs) were observed to lower the energy of the LUMO orbital centered on

---

[a] *Dr. J. M. Aslan, Dr. D. J. Boston, Prof. F. M. MacDonnell*
Chemistry and Biochemistry Department
The University of Texas at Arlington
700 Planetarium Place, Arlington, TX 76019 (USA)
E-mail: macdonn@uta.edu

the dppz ligand in a number of $[ReCl(CO)_3(dppzX_2)]$ analogues, where X = –F, –Cl, and $–CF_3$.[7]

In this work, we explore the electronic ramifications of symmetrically disubstituted dppz analogues, using –Br or –CN electron-withdrawing groups. Our goal is to prepare a ruthenium(II) photocatalyst which undergoes multi-electron photoreduction in the presence of sacrificial donors, which ideally stores these electrons at potentials useful for proton reduction. Finally, it was hoped the positioning of these substituents would hinder radical dimerization side reactions.

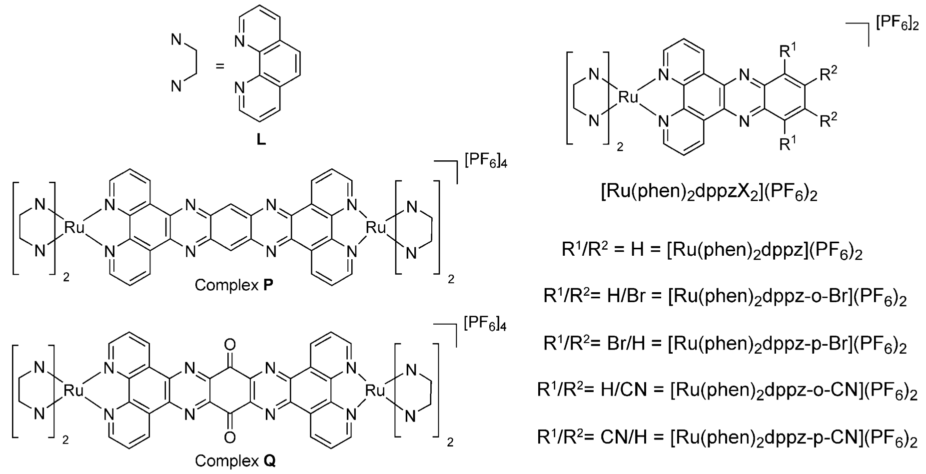

Figure 1. Complexes discussed in this work.

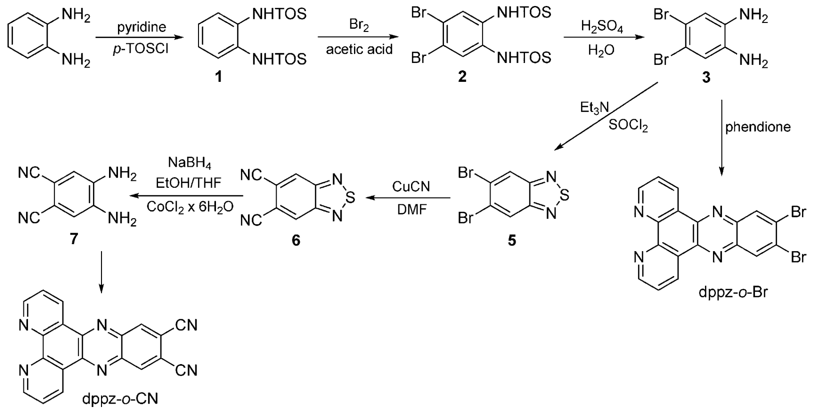

Figure 2. Synthetic route towards the 11,12-disubstituted dppz analogues.

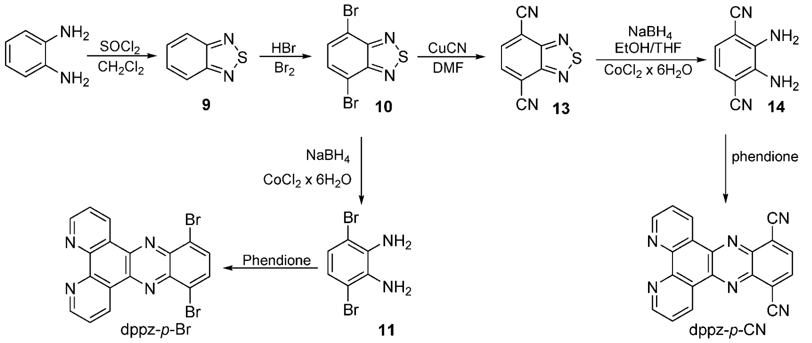

Figure 3. Synthetic route towards the 10,13-disubstituted dppz analogues.

Results and Discussion

Synthesis of $dppzX_2$ and $[Ru(phen)_2(dppzX_2)]^{2+}$ analogues

The synthetic preparation of the materials used for these studies are shown schematically in Figure 1, Figure 2, Figure 3. The preparation of dppz-*o*-Br and dppz-*p*-Br were previously reported.[8] The preparation of dicyano derivatives is new, as is the complexation of these four acceptor ligands to a Ru^{II} ion. All of the dppz acceptor ligands were prepared by a condensation reaction between 1,10-phenanthroline-5,6-dione (phendione) and the corresponding disubstituted 1,2-phenylenediamines. In cases where a sulfur-extrusion was necessary to deprotect the diamino substituents, a Co^{II}/$NaBH_4$ reduction system designed by Neto et al. was used, to afford the diamines in relatively high yields.[8e,f] Both dicyano substituted 1,2-phenylenediamines were prepared from their respective dibromo 1,2-phenylenediamine analogues using CuCN in DMF.[8d,9] The yields of dppz-*o*-Br and dppz-*o*-CN ligands from their diamino counterparts 1,2-diamino-4,5-dibromobenzene (**3**) and 1,2-diamino-4,5-dicyanobenzene (**7**), was approximately 82 % and about 78 %, respectively.

^1H NMR spectra of the free-ligand dppz-*o*-Br shows a singlet ($\delta = 8.58$ ppm), corresponding to protons in the 10 and 13 positions of the symmetrical dppz ligand.[8c] When substituting the free-ligand with –CN to afford dppz-*o*-CN, this singlet shifts noticeably ($\delta = 9.03$ ppm). Proton shifting in cyclic aromatic compounds is expected where stronger EWG's may deshield protons, in proportion to the strength of the withdrawing group. In this case, substitution of –CN in place of –Br results in a $\Delta\delta \approx 0.5$ ppm.

A similar effect is observed for substitution of –Br or –CN in the 10 and 13 positions of dppz. ^1H NMR spectra of dppz-*p*-Br shows a singlet ($\delta = 8.00$ ppm), corresponding to protons in the 11 and 12 positions of the dppz ligand.[8g] Substitution with the cyano group in the 10,13 positions of the free-ligand affords dppz-*p*-CN and results in a $\Delta\delta \approx 0.6$ ppm, ($\delta = 8.59$ ppm), consistent with the deshielding effect observed in the previous case. Interestingly, the magnitude of downfield proton shifting upon switching from –Br to –CN functionalization is nearly equal in both *ortho*- or *para*-disubstitution examples.

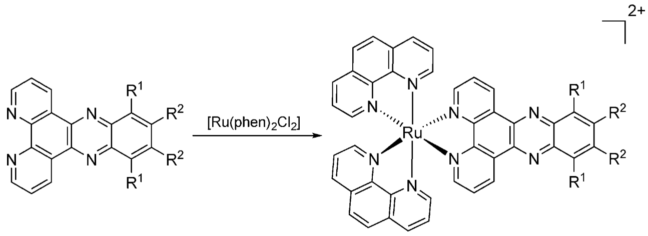

Figure 4. Synthesis of the final complexes by addition of $[Ru(phen)_2Cl_2]$.

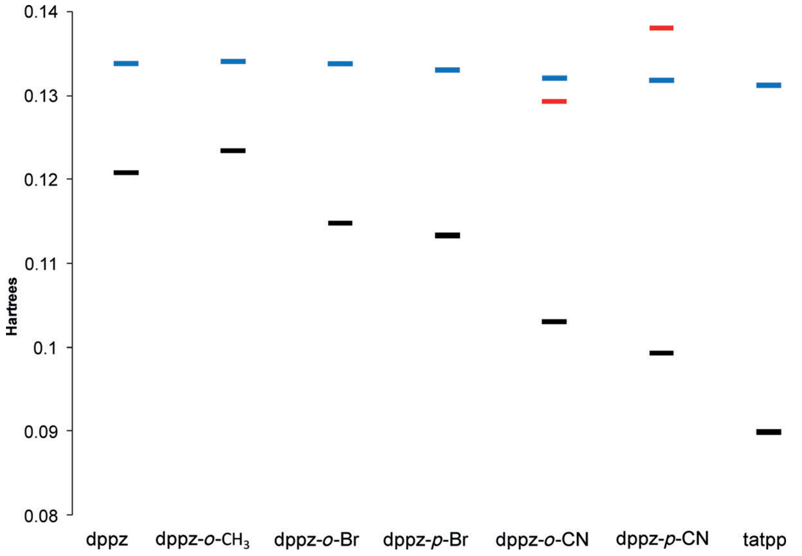

Figure 5. Solvated (MeCN), ground state, DFT calculations (B3LYP level) of Ru^{II}-bound complexes. The HOMO was set to 0 eV for this diagram. LUMO orbitals (black line) represent MO's centered on the pyrazine portion of the dppz or tatpp ligand. LUMO + 1 orbitals (blue line) represent the phen centered MO's for most complexes. In 11,12-dicyanodppz, and 10,13-dicyanodppz, a new dppz centered orbital (red line) is observed.

Calculations

Solvated, ground state DFT calculations of various $[Ru(phen)_2(dppzX_2)]^{2+}$ analogues where X = –H, –CH$_3$, –Br, and –CN, were performed at the B3LYP level using Gaussian 03, using acetonitrile as the solvent.[10] The overall charge of each complex was set to (+2) to account for the Ru^{II} metal. In order to make comparisons between the energies of the LUMO and LUMO + 1 orbitals between various $[Ru(phen)_2(dppzX_2)]^{2+}$ analogues, the Ru dπ-based HOMO was set to 0.0 eV, since the energy of this orbital should remain relatively similar in each complex. The results are shown in Figure 5. In every complex, the LUMO is localized on the dppz or tatpp ligands, shown pictorially in Figure 6. The dppz centered LUMO is typically localized around the phenazine portion of the acceptor ligand. In most complexes, the LUMO + 1 is localized around the 1,10-phenanthroline portion of the complexes, which is commonly referred to as the optical orbital.[11] This is because the MLCT absorption maximum (~450–480 nm) corresponds to the energy gap between the HOMO–LUMO + 1 orbitals, and is nearly identical in both $[Ru(phen)_3]^{2+}$ and $[Ru(bpy)_3]^{2+}$ complexes. A similar phenomena occurs in complexes **P** and **Q**, where neither complex shows significant absorptions below the 480 nm MLCT band. As expected, the data in Figure 4 and Figure 5 show that strong electron-withdrawing groups, such as CN, greatly stabilize the energy of the phenazine (phz) centered dppz orbital (the LUMO), with only minor influence on the LUMO + 1.

Bromo substituents show a modest stabilization of the LUMO orbital. The position of the substituents on the distal ring of the dppz ligand also shows observable differences in orbital energy modifications. Substituting electron-withdrawing groups in the 10,13 positions, shows an enhanced stabilization of the ligand centered orbitals, compared to substitution in the 11,12 positions for the same substituent. Interestingly, it was also noted when –CN is used as a substituent, the MO calculations predict a second ligand centered orbital on both dppz-CN analogues, which is interesting when compared to ligands reported by Pena et al., specifically in regard to how close energetically the second ligand centered orbital lies in contrast to the phen-centered orbitals.[12] The energy of this MO is greatly affected by substituent position, and represents a second orbital localized on the dppz ligand, as shown in Figure 6.

Electrochemistry

Fees et al. have shown the first reduction of $[Ru(bpy)_2(dppz)]^{2+}$ in dry DMF occurs at –0.72 V versus NHE, which corresponds to reduction of the dppz ligand to form the coordinated anion, that is, $[(bpy)_2Ru(dppz^{\bullet-})]^{2+}$.[6a, 13] The second and third reductions of $[Ru(bpy)_2dppz]^{2+}$ occur at –1.15 and –1.35 V versus NHE, and can be attributed to sequential one-electron reductions of the metal bound bpy co-ligands. The second and third reduction potentials differ by approximately 0.16 V, which the authors attribute to coulombic repulsion.

In this work, the electrochemical reduction of $[Ru(phen)_2dppz]^{2+}$ in DMF closely matches the results obtained by Fees et al. as shown in Table 1. The first reduction occurs at –0.72 V versus NHE, with the second and third reductions oc-

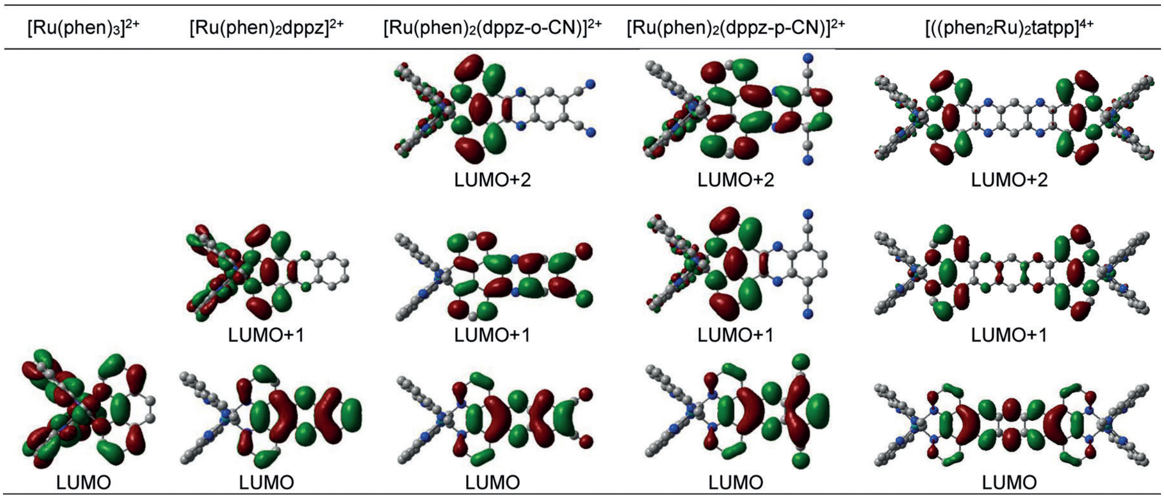

Figure 6. MO pictures for the relevant orbitals described in Figure 5 for the phen, dppz, dppz-*o*-CN, dppz-pCN, and tatpp ligands coordinated to a Ru(phen)$_2$$^{2+}$ unit.

curring at −1.11 and −1.32 V. The first reduction of [Ru(phen)$_2$(dppz-*o*-Br)]$^{2+}$ and [Ru(phen)$_2$(dppz-*p*-Br)]$^{2+}$ is shifted by 190 and 230 mV, respectively, positive to that observed for [Ru(phen)$_2$(dppz)]$^{2+}$, as anticipated by the computational data. The second and third reductions are at potentials more negative than −1.0 V and similar to those seen for [Ru(phen)$_2$dppz]$^{2+}$. Given their values, these are assigned to be one-electron reductions of the metal bound phen ligands.

Conversely, CV and DPV scans of [Ru(phen)$_2$(dppz-*o*-CN)]$^{2+}$ and [Ru(phen)$_2$(dppz-*p*-CN)]$^{2+}$ showed two and three reduction peaks, respectively, in the region between −0.15 and −0.90 V, which are all assigned as dppz-based reductions (Figure 7). The potentials of these processes are listed in Table 1. Two additional reductions at about −1.17 and −1.34 V are seen for both [Ru(phen)$_2$(dppz-*o*-CN)]$^{2+}$ and [Ru(phen)$_2$(dppz-*p*-CN)]$^{2+}$ showing reduction of the terminal phenanthrolines occurs at similar potentials to the other complexes even after multiple reductions of the dppz(CN)$_2$ ligand.

Table 1. Reduction potentials of ruthenium-dppz complexes and related analogues. Reductions of the metal bound phen or bpy ligands are highlighted in bold.

Complexes[a]	^1E [V]	^2E [V]	^3E [V]	^4E [V]	^5E [V]
[Ru(phen)$_3$]$^{2+}$	−1.05	−1.25	−1.5		
[Ru(bpy)$_2$dppz]$^{2+}$ ([1j])	−0.72	**−1.15**	**−1.35**		
[Ru(phen)$_2$dppz]$^{2+}$	−0.72	**−1.11**	**−1.32**		
[Ru(phen)$_2$tatppαRu(phen)$_2$]$^{4+}$ [4]	−0.52[b]	−0.93[b]			
[Ru(phen)$_2$tatppRu(phen)$_2$]$^{4+}$ [4]	−0.01[b]	−0.5[b]			
[Ru(phen)$_2$tatpqRu(phen)$_2$]$^{4+}$ [6b]	0.01[c]	−0.36[c]			
[Ru(phen)$_2$tatppOMeRu(phen)$_2$]$^{4+}$ [5]	−0.05 V	−0.52			
[Ru(phen)$_2$(dppz-*o*-Br)]$^{2+}$	−0.53	**−1.17**[f]	**−1.33**		
[Ru(phen)$_2$(dppz-*p*-Br)]$^{2+}$	−0.49	**−1.18**[f]	**−1.34**		
[Ru(phen)$_2$(dppz-*o*-CN)]$^{2+}$	−0.26	−0.90[e,f]		**−1.16**	**−1.33**
[Ru(phen)$_2$(dppz-*p*-CN)]$^{2+}$	−0.18	−0.5[d,f]	−0.84	**−1.19**	**−1.35**
[Co(Cp(CH$_3$)$_5$)$_2$][14]	−1.3				

[a] Obtained from CV data collected using the hexafluorophosphate salts in N$_2$ purged, dry DMF, with Ag$^+$/Ag reference electrode, Pt counter electrode, and *n*Bu$_4$NPF$_6$ (0.1 M) supporting electrolyte. CVs were run at 50 mV s^{-1} and reduction potentials are reported versus NHE (Fc$^+$/Fc internal reference). [b] Converted to NHE from Ag$^+$/Ag by adding 0.21 V. [c] Converted to NHE from SCE by adding 0.24 V. [d] Non-reversible reduction/oxidation step. [e] Small wave; reversible. [f] Partly irreversible.[15]

Chemical reduction

The electronic absorption spectra of the reduced forms of both dicyano complexes were collected by chemical titration methods and spectroelectrochemical techniques. For the chemical titration data, the optical absorption spectra of the reducing agent [((CH$_3$)$_5$Cp)$_2$Co] must be considered and has been previously reported in acetonitrile solutions.[16] Although the electronic absorption spectra of the 19-electron [(Cp*)$_2$Co] species is featureless above 350 nm, [(Cp*)$_2$Co]$^+$ has small absorptions at 420 nm ($\varepsilon = 330\,\mathrm{M^{-1}\,cm^{-1}}$), 469 nm ($\varepsilon = 8\,\mathrm{M^{-1}\,cm^{-1}}$), 540 nm ($\varepsilon = 0.8\,\mathrm{M^{-1}\,cm^{-1}}$), and 787 nm ($\varepsilon = 0.2\,\mathrm{M^{-1}\,cm^{-1}}$). All of which are essentially negligible relative to the strong LC and MLCT bands with the molar absorptivities of ruthenium–polypyridals ($\varepsilon = 5000\text{–}20\,000\,\mathrm{M^{-1}\,cm^{-1}}$), thus the changes observed are attributed to the Ru complexes. The absorption spectra of the product of the two dicyano complexes upon reaction with one or two equivalents of [(Cp*)$_2$Co] are shown in Figure 8 and Figure 9, respectively. The changes induced by protonation of these reduced species with one or two equivalents of trifluoroacetic acid (TFA), is also shown in these Figures. The absorption spectra of [Ru(phen)$_2$(dppz-*o*-CN)]$^{2+}$ shows two peaks at 380 and 440 nm which are assigned to a ligand-centered n-π* transition and a MLCT (d-π*) transition. The fact that the energy (peak position) of the MLCT band is unchanged relative to [Ru(phen)$_3$]$^{2+}$ is evidence that this transition is from the Ru$^{\mathrm{II}}$ metal and the LUMO+1 orbital. This feature of the lowest energy optical transition being associated with an orbital other than the ligand centered LUMO, is the defining characteristic of laminate

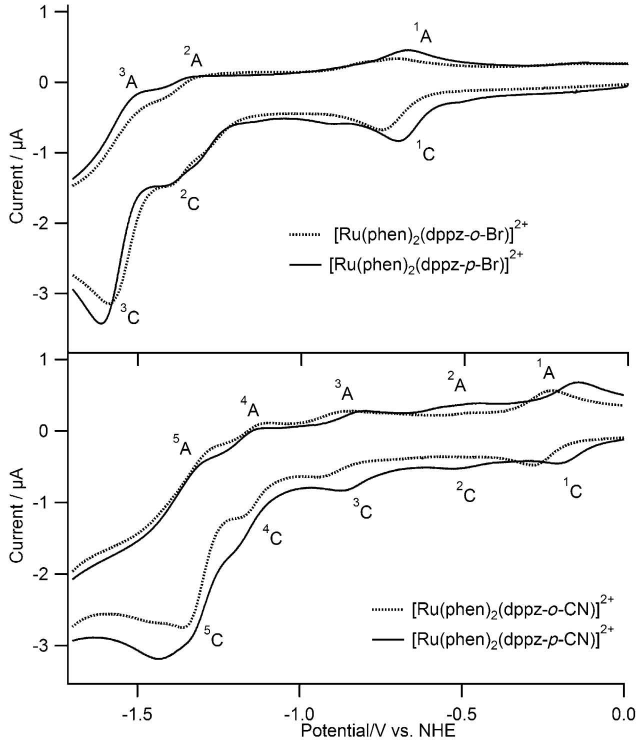

Figure 7. CV scans in dry DMF using Ag/Ag$^+$ reference electrode, *n*Bu$_4$NPF$_6$ (0.1 M) supporting electrolyte, glassy carbon (1.5 mm I.D.) working electrode, and Pt counter electrode with a scan rate of 50 mVs^{-1}. [Ru(phen)$_2$(dppz-*o*-Br)]$^{2+}$ and [Ru(phen)$_2$(dppz-*p*-Br)]$^{2+}$ (top) and [Ru(phen)$_2$(dppz-*o*-CN)]$^{2+}$ and [Ru(phen)$_2$(dppz-*p*-CN)]$^{2+}$ (bottom). Potentials reported versus NHE.

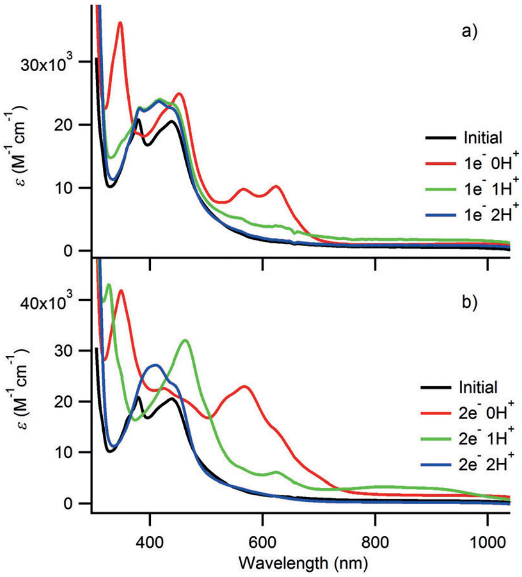

Figure 8. Spectral changes of [Ru(phen)$_2$(dppz-*o*-CN)]$^{2+}$ upon chemical reduction and protonations using [(Cp*)$_2$Co] as the reducing agent, and trifluoroacetic acid as the proton source. All samples were prepared under N$_2$ atmosphere in a glove-box. a) Protonations of the singly reduced complex. b) Protonations of the doubly reduced complex.

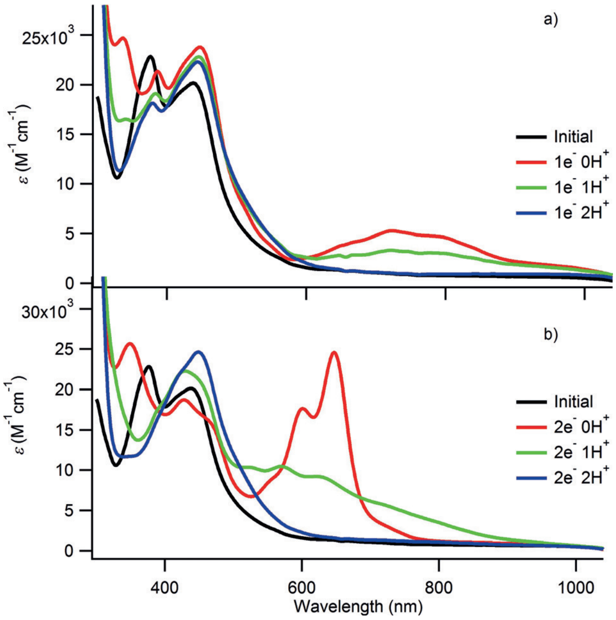

Figure 9. Spectral changes of [Ru(phen)$_2$(dppz-*p*-CN)]$^{2+}$ upon chemical reduction and protonations using [(Cp*)$_2$Co] as the reducing agent, and trifluoroacetic acid as the proton source. All samples were prepared under N$_2$ atmosphere in a glove-box. a) Protonations of the singly reduced complex. b) Protonations of the doubly reduced complex.

acceptor ligands.[6b, 11d] When reduced by one electron, the resulting [Ru(phen)$_2$(dppz-*o*-CN$^{\bullet-}$)]$^+$ complex shows new absorption bands at 347, 566 and 624 nm. The latter two are likely new LC bands associated with the electron now stored in the LUMO of the starting complex. The band at 347 nm seems to be a blue shifting of the 380 nm n-π* band from the starting complex. Notably, the MLCT band, now at 457 nm is largely unperturbed except for an increase in intensity and a slight red-shift. This provides further support that the transition to the LUMO + 1 is only modestly changed by partial occupation of the LUMO.

As shown in Figure 10, spectroelectrochemistry of [Ru(phen)$_2$(dppz-*o*-CN)]$^{2+}$ in dry MeCN shows similar, though less pronounced, changes in the optical spectrum. Protonation of the chemically reduced species bleaches the 566 and 624 nm peaks, ultimately leaving a complex structured band of peaks in the 380–460 nm region (Figure 8 a). We are unsure of what is happening in these circumstances, as single protonation of the singly reduced [(phen)$_2$Ru(tatpp$^{\bullet-}$)Ru(phen)$_2$]$^{3+}$ and [(phen)$_2$Ru(tatpp$^{\bullet-}$)]$^+$ complexes have previously been shown to undergo disproportionation.[17] The data here do not clearly reveal the products.

The initial absorption spectra of [Ru(phen)$_2$(dppz-*p*-CN)]$^{2+}$ are similar to [Ru(phen)$_2$(dppz-*o*-CN)]$^{2+}$, and the band assignments are the same. In this case, reduction by one electron results in the Ru(phen)$_2$(dppz-*p*-CN$^{\bullet-}$)]$^+$ complex, with a broad slightly structured band between 600–900 nm (Figure 9 a). This behavior is reminiscent of the optical features seen upon 1-electron reduction of [(phen)$_2$Ru(tatpp$^{\bullet-}$)Ru(phen)$_2$]$^{3+}$ and [(phen)$_2$Ru(tatpp$^{\bullet-}$)]$^+$.[18] Again the MLCT band is only modestly perturbed by the reduction, showing the newly stored electron is not located in the acceptor orbital for the optical transition. Addition of one proton equivalent decreases the absorption

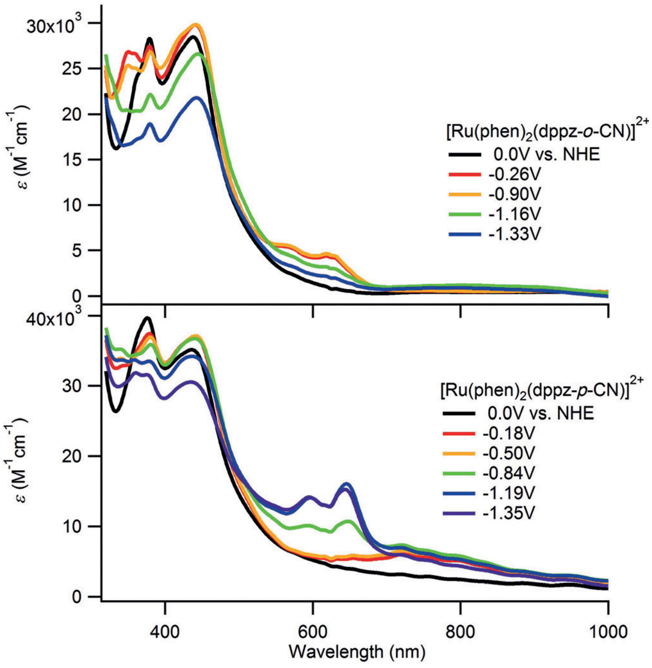

Figure 10. Spectroelectrochemistry of complex [Ru(phen)$_2$(dppz-*o*-CN)]$^{2+}$ (top) and [Ru(phen)$_2$(dppz-*p*-CN)]$^{2+}$ (bottom) in argon purged MeCN using Ag+/Ag reference electrode, Pt counter electrode, gold mesh working electrode with nBu$_4$NPF$_6$ (0.1 M) supporting electrolyte. Potentials listed in the Figure were referenced to CV data in DMF for clarity.

bands between 600–900 nm and 337 nm, consistent with a disproportionation mechanism to [Ru(phen)$_2$(dppz-*p*-CN)]$^{2+}$ and [Ru(phen)$_2$(H$_2$dppz-*p*-CN)]$^{2+}$ (where H$_2$dppz-*p*-CN is the double reduced and doubly protonated form of the ligand). This behavior also mirrors what is observed upon protonation of [(phen)$_2$Ru(tatpp$^{\bullet-}$)Ru(phen)$_2$]$^{3+}$ and [(phen)$_2$Ru(tatpp$^{\bullet-}$)]$^{+}$ complexes.[18] Addition of a second proton equivalent completely bleaches the broad band, completing the disproportionation reaction.

Double reduction to [Ru(phen)$_2$(dppz-*p*-CN^{2-})] results in the growth of a structured absorption band with three peaks at 550, 600, and 647 nm and still only modestly perturbs the MLCT band. Adding one proton equivalent to this [Ru(phen)$_2$(dppz-*p*-CN^{2-})] dianion results in broadening of the band between 500–720 nm, and an increase in the absorbance at 450 nm. Addition of the second proton converts the complex completely to [Ru(phen)$_2$(H$_2$dppz-*p*-CN)]$^{2+}$ which is characterized by a strong LC band overlapping with the MLCT band at approximately 450 nm. Spectroelectrochemistry of [Ru(phen)$_2$(dppz-*p*-CN)]$^{2+}$ in dry MeCN similarly shows first a broad band out around 750 nm, followed by a structured band with peaks between 580 and 700 nm (Figure 10b).

Photoreduction of [Ru(phen)$_2$(dppz-*o*-CN)]$^{2+}$ and [Ru(phen)$_2$(dppz-*p*-CN)]$^{2+}$

The ability to singly reduce the dppz-*o*-CN and dppz-*p*-CN ligands in [Ru(phen)$_2$(dppz-*o*-CN)]$^{2+}$ and [Ru(phen)$_2$(dppz-*p*-CN)]$^{2+}$ complexes without bleaching the fundamental MLCT transition, is the key to allowing such complexes to store multiple electrons under reductive quenching conditions during photolysis. As shown in Figure 11 and Figure 12, the optical changes observed for [Ru(phen)$_2$(dppz-*o*-CN)]$^{2+}$ and [Ru(phen)$_2$(dppz-*p*-CN)]$^{2+}$ upon irradiation with 470 nm light in the presence of 0.2 M triethylamine are consistent with two sequential one-electron reductive quenchings of the photoexcited Ru complexes, as indicated in Figure 13 (reaction 1).

The spectrum of the final products suggests both complexes have been doubly reduced, but only singly protonated. This is consistent with the types of products seen in the tatpp based photochemistry in MeCN with 0.2 M TEA.[3] While the resonance structure of the anionic ligand shown in reaction 1 (Figure 13, right) would likely be basic, this is just one of many resonance structures, where basicity of these nitrogen atoms has been

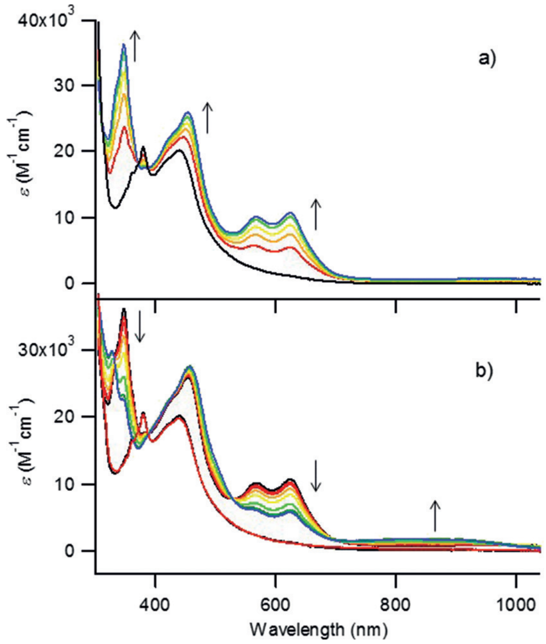

Figure 11. Photoreduction of [Ru(phen)$_2$(dppz-*o*-CN)]$^{2+}$ (50 µM) in N$_2$ purged MeCN (3.0 mL ttl. volume) with TEA (0.2 M), using 470 nm light. a) First observed photoprocess. b) Second observed photoprocess.

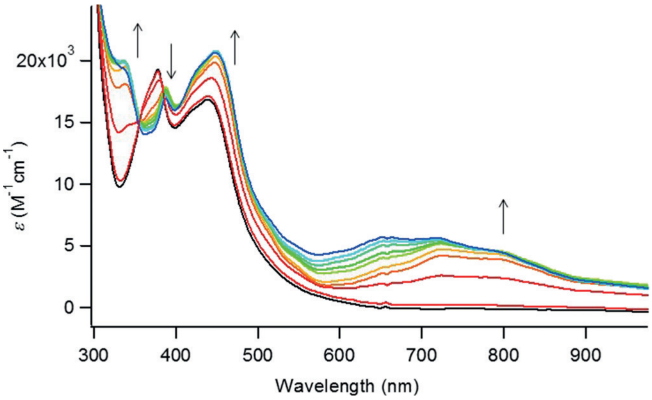

Figure 12. Photoreduction of [Ru(phen)$_2$(dppz-*p*-CN)]$^{2+}$ (50 µM) in N$_2$ purged MeCN (3.0 mL total volume) with TEA (0.2 M), using 470 nm light.

shown to be quite modest for the related tatpp-based anions.[3,17] The reaction is conducted in dry MeCN and therefore the only source of protons is through the decomposition of the TEA radicals generated upon reductive quenching (Figure 13, reaction 2).[19]

While many of the TEA cations may decompose as shown in reaction 2, pathways exist which do not release protons. Because of the nature of the sacrificial donor, it is possible the radical intermediates produced during decay of the TEA radical cation (reaction 2), are providing the second reducing equivalent for the complexes under study. In this case, a single photonic event could net a two electron reduction of the Ru complex. To further examine this possibility, we followed several photolysis reactions by their absorption spectra and stopped the irradiation just after the first reduction finished and the second process was becoming apparent. The spectral changes stopped when the irradiation stopped. After standing in the dark for 2 min, the irradiation was restarted upon which the spectral changes continued as in prior continuous irradiation experiments. The same final spectrum was obtained. As the TEA radicals are short-lived, the 2 min dark period is used to remove all such species from solution in situations where the only ruthenium species present are singly and some doubly reduced products. The photoreactivity of this solution is evidence that the second reduction in the two dicyano complexes can be photochemically driven.

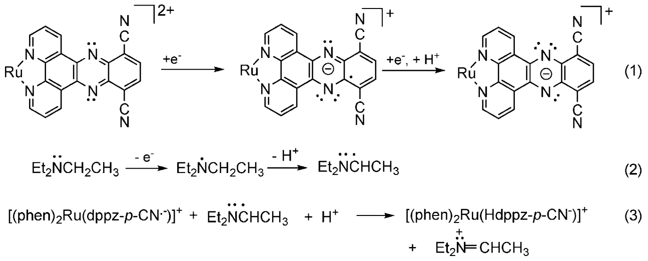

Figure 13. Reaction schemes for sequential reduction of dppz-*p*-CN (1), TEA decomposition (2), and photolysis products (3).

This is not to say that thermal reduction of ruthenium complexes by the TEA radical does not occur during photolysis, only that it is a side reaction which if absent, would not prevent the net two photon, two-electron reduction of [Ru(phen)$_2$(dppz-*o*-CN)]$^{2+}$ and [Ru(phen)$_2$(dppz-*p*-CN)]$^{2+}$. In other words, the Ru dπ-phen π* MLCT manifold in the singly reduced [Ru(phen)$_2$(dppz-*o*-CN$^{\bullet-}$)]$^{+}$ and [Ru(phen)$_2$(dppz-*p*-CN$^{\bullet-}$)]$^{+}$ is still functional to generate a triplet excited state that is long-lived enough to undergo reductive quenching, leading to a second reduction of the dicyanodppz ligands. We would argue that the rare ability of these tatpp and dicyanodppz complexes to undergo multiple photoreductions is because the initial electron is stored in the lower-lying redox-orbital (LUMO) and not the optical "phen-like" orbital (LUMO+1 or LUMO+2). The resulting complex is then still functional photochemically through a traditional excitation into the MLCT manifold.

Conclusion

Modification of the dppz ligand with two cyano substituents expands the ligands π-conjugation and inserts strong electron-withdrawing groups (EWG), which results in the ligands ability to store multiple electrons upon photoexcitation when incorporated into a ruthenium(II) complex. Substitution with the EWG bromo substituents alone was not enough to impart this multi-electron storage capacity. The cyano modifications are shown to stabilize the phenazine-based LUMO, with the 10,13-substitution showing greater stabilization over the 11,12-substitution. The ruthenium complexes with these new ligands are capable of storing up to two photochemically excited electrons in this stabilized MO at approximately 0.2 to 0.3 V more negative than seen in **P** and **Q**, reflecting an increase in stored energy. We are exploring pathways to further store this energy in a fuel, such as H_2, to establish a photocatalytic fuel-forming reaction.

Experimental Section

Materials and reagents

o-Phenylenediamine (Acros, CAS: 95-54-5), HBr (48%, Fluka, CAS: 10035-10-6), Br_2 (99.8% Alfa Aesar, CAS: 7726-95-6), Et_3N (99.5%, SigmaAldrich, CAS: 121-44-8), $SOCl_2$ (SigmaAldrich, CAS: 7719-09-7), CuCN (Fluka, CAS: 544-92-3), $NaBH_4$ (SigmaAldrich, CAS: 16940-66-2), NH_4PF_6 (Oakwood Products, CAS: 16941-11-0), $FeCl_3{\cdot}6H_2O$ (Acros, CAS: 7705-08-0) were purchased and used without further purification. 1,10-Phenanthroline-5,6-dione (phendione) was synthesized according to literature procedures.[6b] [Ru(phen)$_2$Cl$_2$] was prepared according to literature procedures.[14] All synthetic reactions were performed under aerobic conditions unless otherwise specified. All solvents were used without further purification unless otherwise noted. Synthesis of compounds **2** and **3** were performed according to literature procedures.[6b,8b,20]

Instrumentation

^{1}H NMR spectroscopic measurements were obtained on a JEOL 500 or 300 MHz spectrometer. IR spectra were obtained using a Bruker Vector 22 FT-IR spectrometer with KBr discs. ESI-MS data were collected using a Thermo Scientific ESI-IT-MS, LCQ DECA-XP, with a flow rate between 5–10 μL min^{-1}, and voltage setting of 4.5 kV.

Cyclic voltammetry (CV) and differential pulse voltammetry (DPV) measurements were performed using CH Instruments (1620 A) electrochemical workstation, with a platinum wire counter electrode, glassy carbon working electrode, and an Ag/AgCl reference electrode. All potentials are reported versus NHE unless otherwise specified. Measurements were performed at room temperature, under N_2, using dry DMF, with nBu$_4$NPF$_6$ (0.1 M) as the supporting electrolyte, and a Ru^{II} complex concentration of (0.05 mM). At the end of the experiments, ferrocene was added to provide an internal reference potential, and the Fc$^+$/Fc couple at 0.64 V versus NHE was used to correct the voltammograms. All potentials are reported versus NHE unless otherwise specified.

Spectroelectrochemistry experiments were performed using both a Hewlett–Packard HP8453A and the CH Instruments (1620A) electrochemical workstation simultaneously, to collect UV/Vis and electrochemical data. The spectroelectrochemical cell kit was purchased from BASi (EF-1351), which included a thin layer quartz cuvette (1 mm pathlength), gold-mesh minigrid working electrode, platinum wire counter electrode, and an Ag/AgCl reference electrode. All spectroelectrochemical experiments were performed using anhydrous MeCN, with $n\mathrm{Bu_4NPF_6}$ (0.1 M) as the supporting electrolyte, and a $\mathrm{Ru^{II}}$ complex concentration of (0.5 mM).

Photoreduction of complexes $[\mathrm{Ru(phen)_2(dppz\text{-}\mathit{o}\text{-}CN)}]^{2+}$ and $[\mathrm{Ru(phen)_2(dppz\text{-}\mathit{p}\text{-}CN)}]^{2+}$ were performed in septum sealed, 1 cm glass cuvettes (Starna). Samples were irradiated with a custom diode light source which emits blue light ($\lambda_{\max} = 470$ nm), described previously.[21] Optimal spectra were recorded on a Hewlett–Packard 8453 UV–visible spectrophotometer.

Chemical reductions and protonations were performed under N_2 atmosphere in dry acetonitrile, with decamethyl cobaltocene $[\mathrm{(Cp^*)_2Co}]$ as the reducing agent and trifluoroacetic acid (TFA) as the proton source. Saturated solutions of decamethyl cobaltocene were prepared in a glove-box under anaerobic conditions, and subsequently filtered. The concentration of the stock solution was determined by adding a known volume to a concentrated sample of $[\mathrm{[MV](PF_6)_2}]$ in dry acetonitrile, (where $[\mathrm{MV}]^{2+}$ is 1,1′-dimethyl-4,4′-bipyridinium or methyl viologen) and quantifying the concentration of the $[\mathrm{MV^{\bullet}}]^{+}$ generated, using the literature reported molar absorptivity values of ε (396 nm) = 41 500 $\mathrm{M^{-1}\,cm^{-1}}$ and ε (608 nm) = 13 500 $\mathrm{M^{-1}\,cm^{-1}}$.[22]

Synthesis

11,12-Dibromodipyrido-[3,2-a:2′,3′-c]phenazine

Synthesis was preformed according to literature procedure.[8c] Phendione, (0.300 g, 1.42 mmol) was suspended in EtOH (50 mL) with K_2CO_3 (0.200 g, 1.44 mmol), with 1,2-diamino-4,5-dibromobenzene (**3**; 0.380 g, 1.42 mmol). The solution was refluxed under N_2 for 12 h. The slurry was filtered using a 0.2 μm nylon membrane. The filter cake was washed with hot H_2O (100 mL), acetone (50 mL), and Et_2O (20 mL) then dried in vacuo at 50 °C for 12 h. Yield 0.512 g (82 %). ^{1}H NMR (500 MHz, $\mathrm{Zn(BF_4)_2}$, [D$_3$]MeCN): δ = 8.23 (dd, J = 4.6, 13.2 Hz, 2 H), 8.58 (s, 2 H), 9.22 (d, J = 6.9 Hz, 2 H), 9.65 ppm (d, J = 9.7 Hz, 2 H).

[Ru(phen)$_2$(11,12-dibromodipyrido-[3,2-a:2′,3′-c]phenazine)](PF$_6$)$_2$

$\mathrm{[Ru(phen)_2Cl_2]}$ (0.119 g, 0.225 mmol) and dppz-*o*-Br (0.110 g, 0.250 mmol) were added to EtOH (30 mL) and H_2O (30 mL). The solution was refluxed under N_2 for 68 h, filtered and NH_4PF_6 (0.15 g, 0.89 mmol) was added to the filtrate. A red precipitate was formed which was filtered and the solid washed with H_2O (50 mL) and diethyl ether (50 mL) and dried in vacuo at 50 °C for 12 h. Yield 0.219 g (82 %). ^{1}H NMR (500 MHz, [D$_3$]MeCN): δ = 7.62 (m, 4 H), 7.74 (dd, J = 5.4, 13.8 Hz, 2 H), 7.99 (d, J = 6.8 Hz, 2 H), 8.09 (d, J = 6.3 Hz, 2 H), 8.19 (d, J = 6.9 Hz, 2 H), 8.24 (s, 4 H), 8.59 (t, J = 7.5, 6.8 Hz, 4 H), 8.79 (s, 2 H), 9.52 ppm (d, J = 9.2 Hz, 2 H). CHN ESI-MS: $[M-2\,\mathrm{(PF_6)}]^{2+}$: calcd: 450.5 m/z, found: 450.536; elemental analysis calcd (%) for [Ru(phen)$_2$(11,12-dibromodipyrido-[3,2-a:2′,3′-c]phenazine)](PF$_6$)$_2$·H$_2$O ($\mathrm{C_{42}H_{26}Br_2F_{12}N_8OP_2Ru}$): C 41.71, H 2.17, N 9.26; found: C 41.55, H 1.80, N 9.29.

5,6-Dibromo-2,1,3-benzothiadiazole (5), 5,6-dicyano-2,1,3-benzothiadiazole (6), and 1,2-diamino-4,5-dicyanobenzene (7)

The synthesis of compounds **5** and **6** were previously reported.[8d] Sulfur extrusion from **6** using NaBH$_4$/EtOH as the reducing system, was reported to give **7** in 53 % yield. Due to the difficulty in reductive desulfurization of substituted diaminobenzene derivatives, research shows $\mathrm{CoCl_2{\cdot}6\,H_2O}$ can be used as a reductive catalyst in NaBH$_4$/EtOH systems, improving yields and reaction time.[8e] Adopting this procedure, **7** was prepared by stirring **6** (1.86 g, 10.0 mmol), in EtOH (100 mL) and THF (10 mL) with $\mathrm{CoCl_2{\cdot}6\,H_2O}$ (0.237 g, 0.996 mmol). The suspension was stirred for 15 min, then NaBH$_4$ (1.89 g, 50.0 mmol) was added in one portion. The mixture was refluxed for 1.5 h, then NaBH$_4$ (0.750 g, 20.0 mmol) was added in one portion to the hot solution. After 30 min the flask was cooled, and filtered through a bed of Celite. The solvent was removed using a rotovap, and the residue was dissolved in H_2O (100 mL). The product was extracted with CH_2Cl_2 (3 × 100 mL), and the organic extracts were combined and dried with MgSO$_4$. The organic extracts were filtered and the solvent removed to give **7**, which was used immediately in the next step. Yield 1.32 g (84 %).

11,12-Dicyanodipyrido-[3,2-a:2′,3′-c]phenazine

Synthesis was preformed according to literature procedures.[8a] 1,2-Diamino-4,5-dicyanobenzene (**7**; 1.32 g, 3.97 mmol) was suspended with phendione (0.834 g, 3.97 mmol) in EtOH (50 mL) with K_2CO_3 (0.400 g, 2.88 mmol) and refluxed under N_2 for 24 h. The slurry was filtered and the filter cake was washed with hot H_2O (100 mL), acetone (50 mL), and diethyl ether (20 mL) then dried in vacuo. Yield 1.02 g (78 %). ^{1}H NMR (500 MHz, $\mathrm{Zn(BF_4)_2}$ [D$_3$]MeCN): δ = 8.29 (dd, J = 5.2, 2.7 Hz, 2 H), 9.03 (s, 2 H), 9.26 (d, J = 6.3 Hz, 2 H), 9.83 ppm (d, J = 9.7 Hz, 2 H). IR (KBr): $\tilde{\nu}$ = 2250 cm^{-1} (CN stretch)

[Ru(phen)$_2$(11,12-dicyanodipyrido-[3,2-a:2′,3′-c]phenazine)](PF$_6$)$_2$

$\mathrm{[Ru(phen)_2Cl_2]}$ (0.119 g, 0.225 mmol) and (dppz-*o*-CN) (0.083 g, 0.250 mmol) were added to EtOH (30 mL) and H_2O (30 mL). The solution was refluxed under N_2 for 72 h and then filtered hot. An aqueous solution of NH_4PF_6 (0.15 g, 0.89 mmol) in water (3 mL) was added to the filtrate, causing immediate precipitation of a brown solid. The mixture was filtered and the solid was washed with 50 mL H_2O (50 mL) and 50 mL diethyl ether (50 mL) and dried in vacuo for 24 h. Yield 0.227 g (93 %). CHN ^{1}H NMR (500 MHz, [D$_3$]MeCN): δ = 7.63 (m, 4 H), 7.77 (dd, J = 5.4, 2.9 Hz, 2 H), 7.98 (d, J = 5.2 Hz, 2 H), 8.14 (d, J = 5.2 Hz, 2 H), 8.18 (d, J = 4.0 Hz, 2 H), 8.24 (s, 4 H), 8.60 (t, J = 7.5, 9.2 Hz, 4 H), 9.07 (s, 2 H), 9.56 ppm (d, J = 9.7 Hz, 2 H). IR (KBr): $\tilde{\nu}$ = 2250 cm^{-1} (CN stretch); ESI-MS: $[M-2\,\mathrm{(PF_6)}]^{2+}$: calcd: 396.9 m/z, found: 397.0; elemental analysis calcd (%) for [Ru(phen)$_2$(11,12-dicyanodipyrido-[3,2-a:2′,3′-c]phenazine)](PF$_6$)$_2$·2 H$_2$O ($\mathrm{C_{44}H_{28}F_{12}N_{10}O_2P_2Ru}$): C 47.20, H 2.52, N 12.51; found: C 47.36, H 2.35, N 12.08.

2,1,3-Benzothiadiazole (9), 4,7-dibromo-2,1,3-benzothiadiazole (10), 1,2-diamino-3,6-dibromobenzene (11), and 10,13-dibromodipyrido-[3,2-a:2′,3′-c]phenazine

The synthesis of compounds **9**, **10**, and **11** were previously reported.[8e,f] Synthesis of **11** was performed according to literature methods using $\mathrm{CoCl_2{\cdot}6\,H_2O}$ as a reductive catalyst with NaBH$_4$/EtOH, and immediately used to synthesize (dppz-*p*-Br) according to literature procedures.[8g] Compound (**11**; 1.32 g, 5.00 mmol) was added to phendione (1.06 g, 5.02 mmol) and K_2CO_3 (0.400 g, 2.88 mmol) in EtOH (50 mL) and refluxed under N_2 for 12 h. The slurry was filtered and the filter cake was washed with hot H_2O (100 mL), acetone (50 mL), and diethyl ether (20 mL). The filter cake was dried in vacuo. Yield 1.89 g (86 %). ^{1}H NMR (500 MHz, $\mathrm{Zn(BF_4)_2}$ [D$_3$]MeCN): δ = 8.00 (s, 2 H), 8.25 (dd, J = 4.7, 13.2 Hz, 2 H), 9.25 (d, J = 6.3 Hz, 2 H), 9.69 ppm (d, J = 8.6 Hz, 2 H).

[Ru(phen)$_2$(10,13-dibromodipyrido-[3,2-a:2′,3′-c]phenazine)]-(PF$_6$)$_2$

[Ru(phen)$_2$Cl$_2$] (0.119 g, 0.225 mmol) and (dppz-*p*-Br) (0.110 g, 0.250 mmol) were added to EtOH (30 mL) and H_2O (30 mL). The solution was refluxed under N_2 for 48 h, and NH_4PF_6 (0.15 g, 0.89 mmol) was added to the filtered solution. A red precipitate formed, which was filtered and washed with H_2O (50 mL) and diethyl ether (50 mL), then dried in vacuo at 50 °C for 24 h. Yield 0.15 g (56 %). ^{1}H NMR (500 MHz, [D$_3$]MeCN): $\delta = 7.63$ (m, 4 H), 7.78 (dd, $J = 5.4$, 13.2 Hz, 2 H), 7.99 (d, $J = 6.3$ Hz, 2 H), 8.13 (d, $J = 6.9$ Hz, 2 H), 8.20 (d, $J = 6.9$ Hz, 2 H), 8.24 (s, 4 H), 8.30 (s, 2 H), 8.60 (t, $J = 8.6$, 8.6 Hz, 4 H), 9.64 ppm (d, $J = 9.2$ Hz, 2 H). ESI-MS: $[M-2(PF_6)]^{2+}$: calcd: 450.75 *m/z*; found: 450.469 *m/z*; elemental analysis calcd (%) for [Ru(Phen)$_2$(10,13-dibromodipyrido-[3,2-a:2′,3′-c]phenazine)](PF$_6$)$_2$·H_2O ($C_{42}H_{24}Br_2F_{12}N_8P_2Ru$): C 41.71, H 2.17, N 9.26; found: C 41.70, H 1.95, N 9.19.

4,7-Dicyano-2,1,3-benzothiadiazole (13)

4,7-Dibromo-2,1,3-benzothiadiazole (**10**; 2.87 g, 9.76 mmol) was added to CuCN (2.84 g, 31.7 mmol) in DMF (40 mL). The slurry was thoroughly degassed with N_2 and refluxed for 3 h. A separate solution of $FeCl_3 \cdot 6H_2O$ (13.0 g, 48.1 mmol) was added to 3.5 mL concentrated HCl (3.5 mL) and H_2O (20 mL). Once the refluxed mixture cooled to RT the $FeCl_3 \cdot 6H_2O$ solution was added to the cooled reaction solution and stirred at 20 °C for 0.5 h. The product was extracted with CH_2Cl_2 (2 × 100 mL) and the combined organic layers were washed with 6 M HCl (3 × 100 mL), H_2O (50 mL), and brine (50 mL). The organic layer was then dried with $MgSO_4$ and the solvent was removed under reduced pressure. Yield 1.12 g (62 %). ^{1}H NMR (500 MHz, [D$_6$]acetone): $\delta = 8.5$ ppm (s, 2 H).

1,2-Diamino-3,6-dicyanobenzene (14)

4,7-Dicyano-2,1,3-benzothiadiazole (1.86 g, 10 mmol) was suspended in EtOH (100 mL) and THF (10 mL) with $CoCl_2 \cdot 6H_2O$ (0.237 g, 1.00 mmol). The suspension was stirred for 15 min, and $NaBH_4$ (1.89 g, 50.0 mmol) was added in one portion. The mixture was refluxed for 1.5 h, and additional $NaBH_4$ (0.750 g, 20.0 mmol) was added in one portion to the hot solution and heated for 0.5 h. The solution was filtered through a bed of Celite and the solvent was removed under reduced pressure. The residue was dissolved in H_2O (100 mL) and extracted with CH_2Cl_2 (3 × 100 mL). The organic extracts were combined, dried with $MgSO_4$ and the solvent was removed under reduced pressure. The crude solid was immediately used in the next step. Yield 1.01 g (64 %)

10,13-Dicyanodipyrido-[3,2-a:2′,3′-c]phenazine

1,2-Diamino-3,6-dicyanobenzene (**14**; 1.01 g, 6.4 mmol) was suspended with phendione (1.34 g, 6.4 mmol) in EtOH (50 mL) with K_2CO_3 (0.4 g, 2.9 mmol) and refluxed under N_2 for 24 h. The slurry was filtered using and the filter cake was washed with 100 mL hot H_2O (100 mL), acetone (50 mL), and diethyl ether (20 mL). The filter cake was dried in vacuo. Yield 1.76 g (83 %). ^{1}H NMR (500 MHz, Zn(BF$_4$)$_2$ [D$_3$]MeCN): $\delta = 8.31$ (dd, $J = 4.8$, 5.7 Hz, 2 H), 8.59 (s, 2 H), 9.29 (d, $J = 6.9$ Hz, 2 H), 9.88 ppm (d, $J = 9.7$ Hz, 2 H); IR (KBr): $\tilde{\nu} = 2250$ cm^{-1} (CN stretch)

[Ru(phen)$_2$(10,13-dicyanodipyrido-[3,2-a:2′,3′-c]phenazine)]-(PF$_6$)$_2$

[Ru(phen)$_2$Cl$_2$] (0.119 g, 0.225 mmol) and (dppz-*p*-CN) (0.083 g, 0.250 mmol) were added to EtOH (30 mL) and H_2O (30 mL). Due to the insolubility of **15** in 1:1 EtOH/H_2O. The solution was refluxed under N_2 for 72 h, filtered, and NH_4PF_6 (0.15 g, 0.89 mmol) was added to the filtered solution. A brown precipitate formed, was filtered, and washed with H_2O (50 mL) and diethyl ether (50 mL), then dried in a vacuo at 50 °C for 24 h. Yield 0.221 g (91 %). ^{1}H NMR (500 MHz, [D$_3$]MeCN): $\delta = 7.63$ (m, 4 H), 7.79 (dd, $J = 5.2$, 2.9 Hz, 2 H), 7.99 (d, $J = 6.3$ Hz, 2 H), 8.176 (d, $J = 6.3$ Hz, 2 H), 8.21 (d, $J = 5.2$ Hz, 2 H), 8.25 (s, 4 H), 8.61 (t, $J = 9.7$, 9.7 Hz, 4 H), 8.63 (s, 2 H), 9.63 ppm (d, $J = 9.7$ Hz, 2 H). IR (KBr): $\tilde{\nu} = 2252$ cm^{-1} (CN stretch); ESI-MS: $[M-2(PF_6)]^{2+}$: calcd: 396.8 *m/z*; found: 397.0; elemental analysis calcd (%) for [Ru(phen)$_2$(10,13-dicyanodipyrido-[3,2-a:2′,3′-c]phenazine)](PF$_6$)$_2$·3 H_2O ($C_{44}H_{30}F_{12}N_{10}O_3P_2Ru$): C 46.45, H 2.66, N 12.31; found: C 46.51, H 2.38, N 11.73.

Acknowledgements

We thank the the National Science Foundation CHE-1301332 and the Robert A. Welch Foundation Y-1301 for financial support. We also thank Dr. Shreeyukta Sing and Mr. Zachary Wu for their assistance and helpful discussions.

Keywords: dppz · multi-electron · photochemistry · ruthenium · storage

[1] a) S. I. Allakhverdiev, V. D. Kreslavski, V. Thavasi, S. K. Zharmukhamedov, V. V. Klimov, S. Ramakrishna, H. Nishihara, M. Mimuro, R. Carpentier, T. Nagata, *Photosynthetic Energy Conversion: Hydrogen Photoproduction by Natural and Biomimetic Means*, Intech, **2010**; b) S. M. Arachchige, J. R. Brown, E. Chang, A. Jain, D. F. Zigler, K. Rangan, K. J. Brewer, *Inorg. Chem.* **2009**, *48*, 1989 – 2000; c) A. J. Esswein, D. G. Nocera, *Chem. Rev.* **2007**, *107*, 4022 – 4047; d) A. Koca, M. Kasimsener, M. Kocak, A. Gul, *Int. J. Hydrogen Energy* **2006**, *31*, 2211 – 2216; e) A. S. Larsen, K. Wang, M. A. Lockwood, G. L. Rice, T.-J. Won, S. Lovell, M. Sadílek, F. Tureček, J. M. Mayer, *J. Am. Chem. Soc.* **2002**, *124*, 10112 – 10123; f) S. Losse, J. G. Vos, S. Rau, *Coord. Chem. Rev.* **2010**, *254*, 2492 – 2504; g) F. M. MacDonnell, *Solar Hydrogen Generation Toward a Renewable Energy Future*, Springer New York, **2008**, p.; h) A. J. Morris, G. J. Meyer, E. Fujita, *Acc. Chem. Res.* **2009**, *42*, 1983 – 1994; i) A. Nada, H. Hamed, M. Barakat, N. Mohamed, T. Veziroglu, *Int. J. Hydrogen Energy* **2008**, *33*, 3264 – 3269; j) S. M. Ng, C. Yin, C. H. Yeung, T. C. Chan, C. P. Lau, *Eur. J. Inorg. Chem.* **2004**, 1788 – 1793; k) J. Olofsson, B. Önfelt, P. Lincoln, *J. Phys. Chem. A* **2004**, *108*, 4391 – 4398; l) K. Sakai, H. Ozawa, *Coord. Chem. Rev.* **2007**, *251*, 2753 – 2766; m) S. Nag, J. G. Ferreira, L. Chenneberg, P. D. Ducharme, G. S. Hanan, G. La Ganga, S. Serroni, S. Campagna, *Inorg. Chem.* **2011**, *50*, 7 – 9; n) K. Kitamoto, K. Sakai, *Angew. Chem. Int. Ed.* **2014**, *53*, 4618—4622; *Angew. Chem.* **2014**, *126*, 4706 – 4710.

[2] a) M. R. Gill, J. A. Thomas, *Chem. Soc. Rev.* **2012**, *41*, 3179 – 3192; b) A. Yadav, T. Janaratne, A. Krishnan, S. S. Singhal, S. Yadav, A. S. Dayoub, D. L. Hawkins, S. Awasthi, F. M. MacDonnell, *Mol. Cancer Ther.* **2013**, *12*, 643 – 653.

[3] a) R. Konduri, T. N. R. de Tacconi, K. Rajeshwar, F. M. MacDonnell, *J. Am. Chem. Soc.* **2004**, *126*, 11621 – 11629; b) R. Konduri, H. Ye, F. M. MacDonnell, S. Serroni, S. Campagna, K. Rajeshwar, *Angew. Chem. Int. Ed.* **2002**, *41*, 3185 – 3187; *Angew. Chem.* **2002**, *114*, 3317 – 3319.

[4] S. Singh, N. R. de Tacconi, N. R. G. Diaz, R. O. Lezna, J. Muñoz Zuñiga, K. Abayan, F. M. MacDonnell, *Inorg. Chem.* **2011**, *50*, 9318 – 9328.

[5] S. Singh, N. R. de Tacconi, D. Boston, F. M. MacDonnell, *Dalton Trans.* **2010**, *39*, 11180 – 11187.

[6] a) J. Fees, W. Kaim, M. Moscherosch, W. Matheis, J. Klima, M. Krejcik, S. Zalis, *Inorg. Chem.* **1993**, *32*, 166 – 174; b) M. J. Kim, R. Konduri, H. Ye,

F. M. MacDonnell, F. Puntoriero, S. Serroni, S. Campagna, T. Holder, G. Kinsel, K. Rajeshwar, *Inorg. Chem.* **2002**, *41*, 2471–2476.

[7] M. K. Kuimova, W. Z. Alsindi, A. J. Blake, E. S. Davies, D. J. Lampus, P. Matousek, J. McMaster, A. W. Parker, M. Towrie, X.-Z. Sun, C. Wilson, M. W. George, *Inorg. Chem.* **2008**, *47*, 9857–9869.

[8] a) J. Rusanova, S. Decurtins, E. Rusanov, H. Stoeckli-Evans, S. Delahaye, A. Hauser, *J. Chem. Soc. Dalton Trans.* **2002**, 4318–4320; b) G. W. H. Cheeseman, *J. Chem. Soc.* **1962**, 1170–1176; c) C. Kuhnt, M. Karnahl, S. Tschierlei, K. Griebenow, M. Schmitt, B. Schafer, S. Krieck, H. Gorls, S. Rau, B. Dietzek, J. Popp, *Phys. Chem. Chem. Phys.* **2010**, *12*, 1357–1368; d) C. Burmester, R. Faust, *Synthesis* **2008**, 1179–1181; e) B. A. DaSilveira Neto, A. S. Lopes, M. Wuest, V. E. U. Costa, G. Ebeling, J. Dupont, *Tetrahedron Lett.* **2005**, *46*, 6843–6846; f) F. S. Mancilha, B. A. DaSilveira Neto, A. S. Lopes, P. F. Moreira, F. H. Quina, R. S. Gonçalves, J. Dupont, *Eur. J. Org. Chem.* **2006**, 4924–4933; g) M. J. Edelmann, J.-M. Raimundo, N. F. Utesch, F. Diederich, C. Boudon, J.-P. Gisselbrecht, M. Gross, *Helv. Chim. Acta* **2002**, *85*, 2195–2213; h) H. M. Gajiwala, R. Zand, *Polymer* **2000**, *41*, 2009–2015.

[9] E. H. Moerkved, S. M. Neset, O. Bjoerlo, H. Kjoesen, G. Hvistendahl, F. Mo, *ChemInform* **1996**, *27*, S137.

[10] Gaussian 03, Revision C.02, M. J. Frisch, G. W. Trucks, H. B. Schlegel, G. E. Scuseria, M. A. Robb, J. R. Cheeseman, J. Montgomery, J. A., T. Vreven, K. N. Kudin, J. C. Burant, J. M. Millam, S. S. Iyengar, J. Tomasi, V. Barone, B. Mennucci, M. Cossi, G. Scalmani, N. Rega, G. A. Petersson, H. Nakatsuji, M. Hada, M. Ehara, K. Toyota, R. Fukuda, J. Hasegawa, M. Ishida, T. Nakajima, Y. Honda, O. Kitao, H. Nakai, M. Klene, X. Li, J. E. Knox, H. P. Hratchian, J. B. Cross, V. Bakken, C. Adamo, J. Jaramillo, R. Gomperts, R. E. Stratmann, O. Yazyev, A. J. Austin, R. Cammi, C. Pomelli, J. W. Ochterski, P. Y. Ayala, K. Morokuma, G. A. Voth, P. Salvador, J. J. Dannenberg, V. G. Zakrzewski, S. Dapprich, A. D. Daniels, M. C. Strain, O. Farkas, D. K. Malick, A. D. Rabuck, K. Raghavachari, J. B. Foresman, J. V. Ortiz, Q. Cui, A. G. Baboul, S. Clifford, J. Cioslowski, B. B. Stefanov, G. Liu, A. Liashenko, P. Piskorz, I. Komaromi, R. L. Martin, D. J. Fox, T. Keith, M. A. Al-Laham, C. Y. Peng, A. Nanayakkara, M. Challacombe, P. M. W. Gill, B. Johnson, W. Chen, M. W. Wong, C. Gonzalez, J. A. Pople, Gaussan, Inc., Wallingford CT, **2004**.

[11] a) A. E. Friedman, J. C. Chambron, J. P. Sauvage, N. J. Turro, J. K. Barton, *J. Am. Chem. Soc.* **1990**, *112*, 4960–4962; b) Y. Sun, C. Turro, *Inorg. Chem.* **2010**, *49*, 5025–5032; c) C. Turro, S. H. Bossmann, Y. Jenkins, J. K. Barton, N. J. Turro, *J. Am. Chem. Soc.* **1995**, *117*, 9026–9032; d) M. B. Majewski, N. R. de Tacconi, F. M. MacDonnell, M. O. Wolf, *Chem. Eur. J.* **2013**, *19*, 8331–8341.

[12] B. Peña, N. A. Leed, K. R. Dunbar, C. Turro, *J. Phys. Chem. C* **2012**, *116*, 22186–22195.

[13] J. Fees, M. Ketterle, A. Klein, J. Fiedler, W. Kaim, *J. Chem. Soc. Dalton Trans.* **1999**, 2595–2600.

[14] P. J. Giordano, C. R. Bock, M. S. Wrighton, *J. Am. Chem. Soc.* **1978**, *100*, 6960–6965.

[15] V. V. Pavlishchuk, A. W. Addison, *Inorg. Chim. Acta* **2000**, *298*, 97–102.

[16] J. L. Robbins, N. Edelstein, B. Spencer, J. C. Smart, *J. Am. Chem. Soc.* **1982**, *104*, 1882–1893.

[17] N. R. de Tacconi, R. O. Lezna, R. Konduri, F. Ongeri, K. Rajeshwar, F. M. MacDonnell, *Chem. Eur. J.* **2005**, *11*, 4327–4339.

[18] a) K. L. Wouters, N. R. de Tacconi, R. Konduri, R. O. Lezna, F. M. MacDonnell, K. L. Wouters, *Photosynth. Res.* **2006**, 87, 41–55; b) N. R. de Tacconi, R. O. Lezna, R. Chitakunye, F. M. MacDonnell, *Inorg. Chem.* **2008**, 47, 8847–8858.

[19] a) P. J. DeLaive, J. T. Lee, H. W. Sprintschnik, H. Abruna, T. J. Meyer, D. G. Whitten, *J. Am. Chem. Soc.* **1977**, *99*, 7094–7097; b) P. J. DeLaive, T. K. Foreman, C. Giannotti, D. G. Whitten, *J. Am. Chem. Soc.* **1980**, *102*, 5627–5631.

[20] T. Kato, H. Masu, H. Takayanagi, E. Kaji, K. Katagiri, M. Tominaga, I. Azumaya, *Tetrahedron* **2006**, *62*, 8458–8462.

[21] D. J. Boston, C. Xu, D. W. Armstrong, F. M. MacDonnell, *J. Am. Chem. Soc.* **2013**, *135*, 16252–16255.

[22] T. M. Bockman, J. K. Kochi, *J. Org. Chem.* **1990**, *55*, 4127–4135.

Received: July 3, 2015